



Emplacement processes and cooling history of layered cyclic unit II-7 from the Lovozero alkaline massif (Kola Peninsula, Russia)

Olivier Féménias^{a,*}, Nicolas Coussaert^b, Stéphane Brassinnes^a, Daniel Demaiffe^a

^aLaboratoire de Géochimie Isotopique et Géodynamique Chimique, DSTE, Université Libre de Bruxelles (CP 160/02),
50, av. Roosevelt, B-1050 Bruxelles, Belgium

^bUnité de Minéralogie et Géochimie, Musée Royal de l'Afrique Centrale, B-3080 Tervuren, Belgium

Received 9 January 2004; accepted 18 February 2005

Available online 25 April 2005

Abstract

The Lovozero alkaline massif (Kola Peninsula, Russia) is composed of three major units. The central unit (80% of the volume) comprises numerous well developed layers composed, from bottom to roof, of an urtite–juvite–foyaite–lujavrite continuous lithological sequence (ijolite–foiid-bearing alkali feldspar syenite in IUGS nomenclature). The mode of emplacement of the massif and the mechanism of formation of the layering are still under debate. Petrological, mineralogical (two stages of crystallisation) and structural evidence from the detailed analysis of one of these layers (unit II-7) is interpreted in terms of both mechanical (magmatic to sub-solidus, non-coaxial deformation) and thermal differentiation operating on a crystal-laden (alkali feldspar, high *T* nepheline, aegirine-augite) material of foyaitic composition. Textural and mineralogical data suggest that a sheet of foiditic magma intruded into solidified earlier units of the Lovozero layered sequence and acquired a sill-like structure on cooling.

© 2005 Elsevier B.V. All rights reserved.

Keywords: Lovozero alkaline massif; Unit II-7; Layered rocks; Sill; Agpaitic syenites

1. Introduction

Since the pioneering work of Wager and co-workers on the Skaergaard intrusion (Wager and Deer, 1939; Wager and Brown, 1968), the origin of layering, and more particularly of cyclic layering, has been hotly debated and many mechanisms have been

proposed (see review books edited by Parsons, 1987 and Cawthorn, 1996). Most of the proposed mechanisms concern ultramafic–mafic layered intrusions (i.e. Skaergaard, Bushveld, Stillwater. . .) that involve classical mineral phases (olivine, ortho- and clinopyroxene, plagioclase, oxides. . .). Highly differentiated alkaline to peralkaline layered intrusions are much less common and are characterised by a specific mineralogy (alkali feldspar, foids, sodic clinopyroxene and/or amphibole, with rare accessory minerals of unusual composition. . .). The Lovozero (Kola Pen-

* Corresponding author. Tel.: +32 2 6502254; fax: +32 2 6502226.

E-mail address: ofemenia@ulb.ac.be (O. Féménias).

insula, Russia; i.e. Gerasimovsky et al., 1966) and Ilimaussaq (Greenland; Larsen and Sorensen, 1987) intrusions are the type-examples of such layered alkaline complexes.

In many papers related to layered intrusions, there are almost no structural nor micro-fabric data published on the layered rocks. However, recent studies in France have developed a micro-fabric approach on both the kinematic analysis of magmatic rocks (Nicolas, 1992; Bouchez et al., 1992) and the experimental aspects of shape fabrics and orientation (Fernandez et al., 1983; Ildefonse and Fernandez, 1988; Ildefonse et al., 1992; Arbaret et al., 1996, 2001).

The Lovozero massif constitutes an exceptional opportunity to study the mode of emplacement and the crystallisation history of an agpaite magma. Agpaite alkaline rocks are rare nepheline syenites characterised by high (>1.2) molar (Na+K)/Al ratio and by the presence of complex Zr- and Ti-silicate minerals (Sørensen, 1997). This paper is focused on one cyclic unit (called the “rhythm II-7”) from the well-layered stratiform central part of the Lovozero massif. Detailed petrological, mineralogical and micro-fabric data were obtained on this cyclic unit to better constrain the crystallisation and cooling history, as well as the development of the layering and of the magmatic fabric within the various lithologies of the cyclic unit (“rhythm”) II-7.

2. Geological setting and structure of the Lovozero massif

The alkaline Lovozero massif is, together with the nearby Khibina (i.e. Kogarko et al., 1995) and the Ilimaussaq layered complex of Greenland (Larsen and Sorensen, 1987), one of the world’s largest occurrences of agpaite nepheline syenite intrusions. It intruded into the Archean to Paleoproterozoic Central Kola Composite Terrane (Kogarko et al., 1995) (Fig. 1a) and was emplaced at 370 ± 7 Ma (whole rock Rb–Sr isochron, Kramm and Kogarko, 1994). Khibina and Lovozero massifs were emplaced in the Proterozoic basement essentially composed of Central Kola trondhjemite–tonalite–granodiorite (TTG) series and various biotite-, hornblende- and pyroxene-gneisses, migmatites and amphibolites of the “basement complex”.

The general geology, mineralogy and geochemistry of Lovozero have been extensively described by Vlasov et al. (1959), Gerasimovsky et al. (1966), Arzamastsev (1994, 1995), Khomyakov (1995) and Pekov (2000). Previous studies and reports (i.e. Kogarko et al., 1995; Arzamastsev et al., 2000 and references below) describe Lovozero as a multi-intrusion complex, interpreted as an asymmetric, stratiform and laccolith-like body. Exposed over a 650 km^2 area between the Umbozero and Lovozero lakes (Fig. 1b), the Lovozero complex is composed of three major intrusive phases:

- 1) The first phase (macro-unit I on Fig. 1b) is composed of poikilitic feldspathoid (nepheline, sodalite and nosean) syenites representing less than 5% of the total volume. This macro-unit constitutes the lower part of the massif, as recognised by drilling, and also tabular sheet-like bodies in the layered central unit. The field relations of these bodies are debatable (Osokin, 1980): for example, do they represent elongated macro-xenoliths or do they belong to the layering? Magmatic breccia containing xenoliths of syenite of this first phase have been observed at the base of the second major phase.
- 2) The second phase (macro-unit II on Fig. 1b) is a well-layered differentiated complex that consists of numerous units (Atamanov et al., 1961 or Gerasimovsky et al., 1966) (Fig. 2a). Arzamastsev (1994) has described a schematic idealised cyclic unit: it consists of an *urtite–juvite–foyaite–lujavrite* continuous series (Fig. 2b). Not all of the layered units are complete; the most complete ones generally occur in the upper part of the layered sequence whereas, in the central and lower parts, lujavritic and foyaitic layers predominate while urtites are generally lacking. According to the IUGS classification (Le Maitre, 2002), these rocks should be named ijolite for urtite, foid syenite for foyaite and foid-bearing alkali feldspar syenite for lujavrite. The layered units have been grouped in 5 series (Atamanov et al., 1961) on the basis of marker horizons (mainly urtite) rich in apatite and/or loparite, from the upper series I to the lower series V that has been reached by drilling at a depth of 1700 m (Fig. 2a). The number of units in each series is

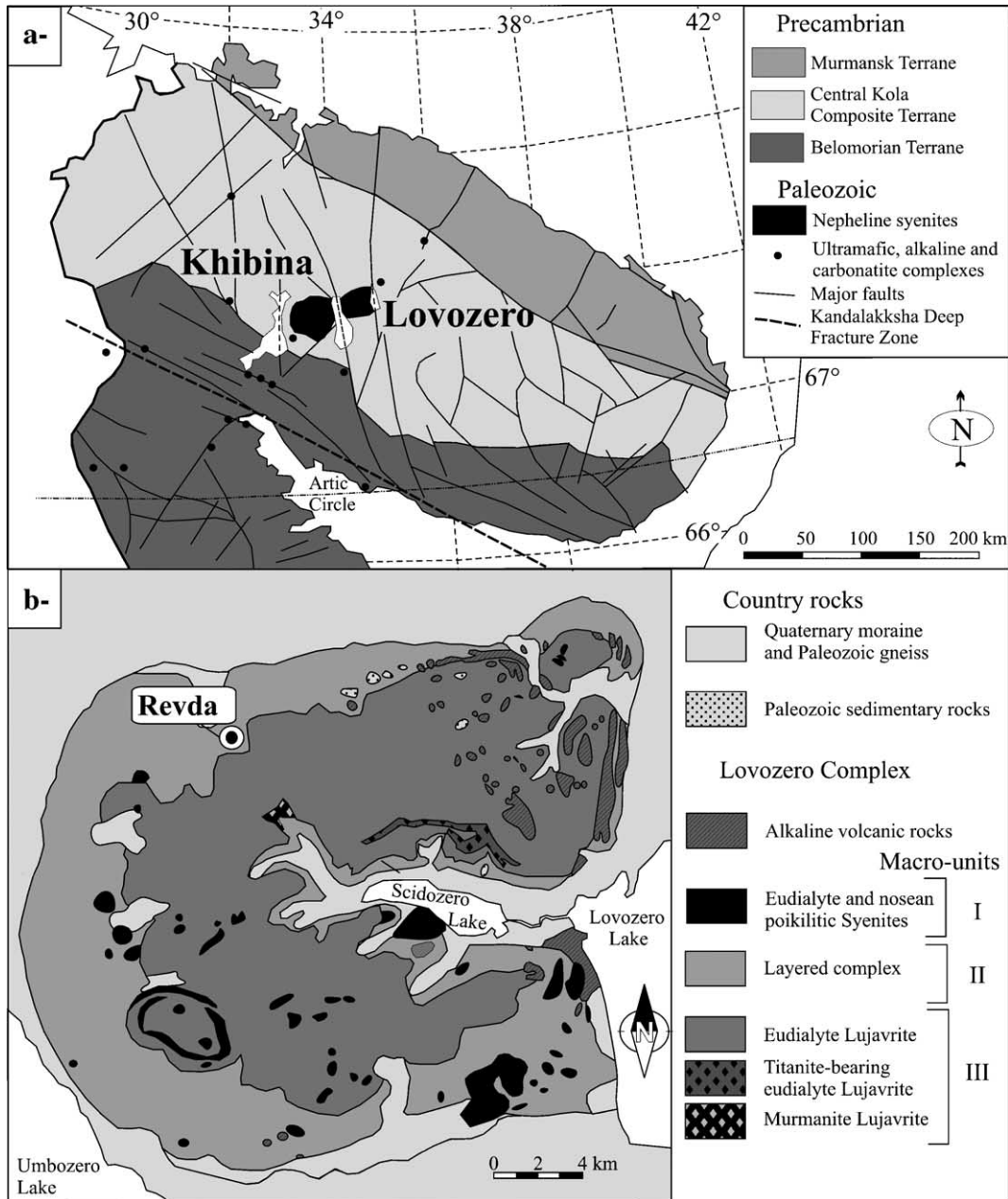


Fig. 1. (a) Simplified sketch map of the Kola Peninsula showing the Precambrian terranes and the Palaeozoic alkaline and carbonatite intrusions (after Kukharensko et al., 1967; Balagansky et al., 1996; Beard et al., 1996). (b) Schematic map of the Lovozero intrusion (modified after Gerasimovskiy et al., 1966; Arzamastsev, 1994). REVDA=quarry from which samples of unit II-7 have been collected.

variable. Geophysical modeling (Arzamastsev et al., 2000) suggests that the apgaitic nepheline syenite variants extend to a depth of 9–10 km. In the border zone of the massif, the layering

disappears and the rock close to the contact with the country rocks is a massive coarse-grained foyaite. In many of the units, the urtite layers, which are good marker horizons, are reduced in

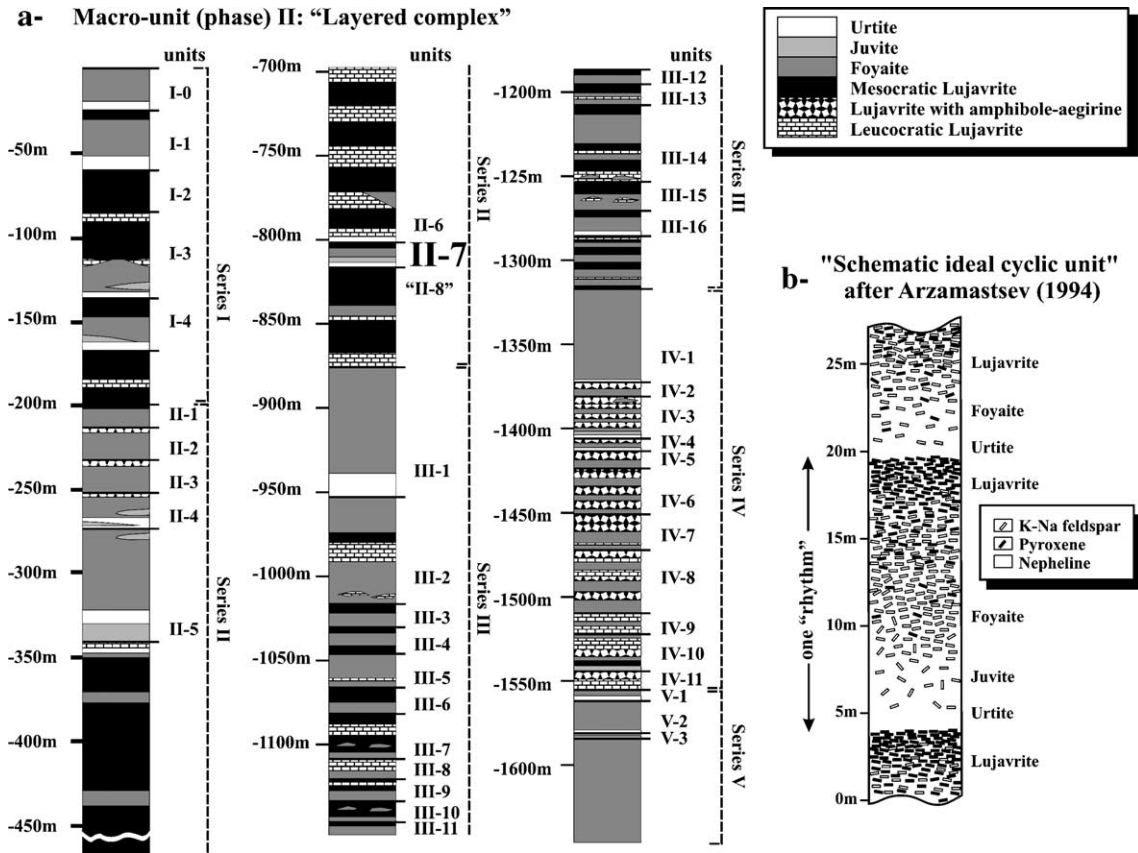


Fig. 2. (a) Stratigraphic cross section of the layered central part of the Lovozero massif showing 5 series (I to V) and the numerous cyclic units (modified from Atamanov et al., 1961; Gerasimovsky et al., 1966). Note that many units do not show the complete sequence urtite–foyaite–lujavrite. (b) Schematic representation of an idealised cyclic unit or “rhythm” (after Arzamastsev, 1994).

thickness to 0.3 m. The local high modal contents of apatite and loparite (up to 10% and 1% respectively) in these horizons have been mined for 50 years. Fieldwork has shown the general absence of steeply inclined cross-cutting relations between the different cyclic units and of real “sedimentary” structures, comparable to those observed in several layered complexes (i.e. Ilimaussaq, Sørensen and Larsen, 1987).

- 3) The third phase (macro-unit III on Fig. 1b) is composed of a eudialyte lujavrite (porphyritic lujavrite to eudialyte lujavrite) that cuts and overlies the two previous phases. At the contact with the layered complex, there is a discontinuous horizon of a fine-grained porphyritic lujavrite containing xenoliths of poikilitic feldspathoid syenite and layered rocks of macro-units I and II.

The lujavrite complex is cut by numerous porphyritic lujavrites containing murmanite and lamprophyllite phenocrysts.

Additionally, rare alkaline ultrabasic rocks have been described (Arzamastsev and Arzamastseva, 1995). Fragments of volcanic (alkaline picrites, ankaramites, alkaline basalts, trachytes and phonolites) and volcano-sedimentary rocks of Devonian age are included in the Lovozero complex especially at its northeastern part (Fig. 1b). The presence of these volcanic xenoliths in the plutonic complex implies a shallow level of emplacement for the complex.

Intrusive contacts with country rocks are clearly marked; they are mainly subvertical (Atamanov et al., 1961; Arzamastsev et al., 2000) except for the western contact where the dipping is about 40° to centre of the

massif. The country rocks are metasomatised over 50–200 m. Near the contact, nepheline syenite dykes and alkaline pegmatites cut across the country rocks.

The three macro-units of the Lovozero massif have been largely sampled (more than 200 samples) but this work is focused on the layered part of the complex (macro-unit II) and more particularly on the complete cyclic unit (or rhythm) II-7. Fifteen samples of this

unit were sampled both from drill cores and from outcrops in the quarry near Revda. This unit has been selected for two main reasons: (1) it has been mined locally for apatite (Revda quarry) so that the field relations with neighbouring units can be easily examined (Fig. 3a) which is not really possible in drill core samples; (2) it shows the ideal complete sequence urtite–juvite–foyaite–lujavrite (Fig. 2b)

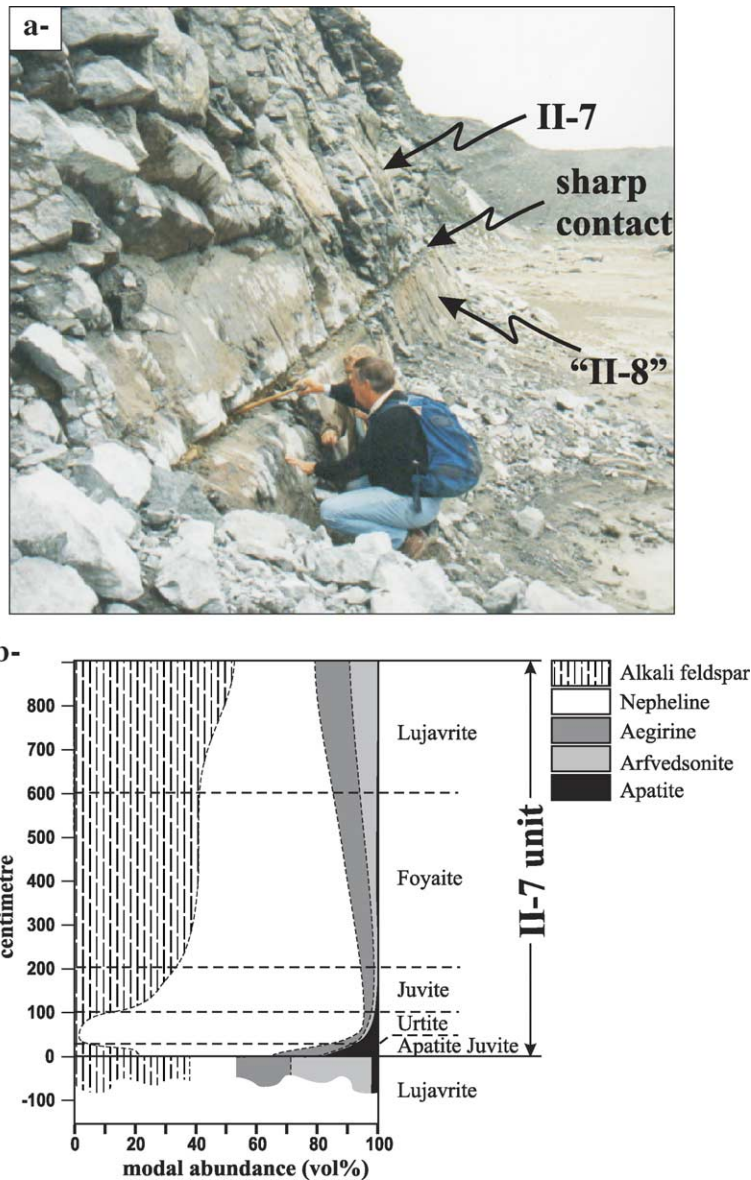


Fig. 3. (a) Sharp contact between the basal apatite-bearing juvite layer of the unit II-7 and the upper lujavrite of the underlying unit "II-8" (quarry near Revda). (b) Qualitative variations of the modal abundances of the principal mineral phases of unit II-7.

described by Arzamastsev (1994) while many other units do not appear as complete. Moreover, it will be shown that each cyclic unit could be related to a distinct magma pulse. The central layered part of Lovozero would then result from the emplacement and differentiation of several magma pulses. In that sense, it would be comparable to the very close Khibina massif that also results from successive phases of intrusion (even if Khibina is not truly a layered intrusion).

3. Petrographic description and deformation features of the rocks of unit II-7

All the rocks of the Lovozero massif, including those of unit II-7 (see Section 3.1) are agpaitic nepheline syenites characterised by euhedral alkali feldspar laths and subhedral to euhedral nepheline surrounded by interstitial ferromagnesian phases. They nevertheless differ in their petrographic textures and modal abundances of the main rock-forming minerals (alkali feldspar, nepheline, Na-rich clinopyroxene and alkali amphibole). These rocks are also characterised by a variety of accessory minerals (Table 1) like sodalite, loparite, eudialyte, apatite, lamprophyllite, lorenzenite (=ramsayite), murmanite and villiaumite, some of them being typical of hyperagpaitic rocks (Khomyakov, 1995).

Although the thickness of the units varies laterally, as observed in drill cores and locally in mined zones, unit II-7, as exposed in the Revda quarry, is about 9 m thick. It is composed of a typical 1 m-thick basal urtite

(ijolite), whose lowermost part (≈ 10 cm) is enriched in apatite and loparite, a juvite (alkali feldspar-bearing ijolite) of similar thickness, a foyaite (foid syenite) (4 m thick) and a lujavrite (foid-bearing alkali feldspar syenite) more than 3 m thick. The modal proportions of alkali feldspar, nepheline, aegirine and arfvedsonite vary gradually from the basal urtite to the overlying juvite, foyaite and lujavrite (Fig. 3b). The contact of the basal urtite of unit II-7 with the underlying lujavrite (unit II-8) is very sharp (Fig. 3, a and b).

3.1. Petrographic description

The *urtites* (i.e. sample Ko 97-92, Fig. 4a) are leucocratic fine- to medium-grained (1–2 mm) rocks. The foliation is poorly marked by the oriented subhedral alkali feldspar laths (5 to 10 vol.%) set in a panidiomorphic assemblage of subhedral to euhedral isometric nepheline (70 to 80 vol.%). Nepheline and alkali feldspar are locally replaced by secondary post-magmatic phases (sodalite and zeolites). The matrix is composed of variable amounts of interstitial poikilitic or prismatic aegirine-augite and euhedral apatite (forming aggregates or included in loparite, aegirine and arfvedsonite). Nepheline commonly contains aegirine and apatite inclusions whereas alkali feldspar is devoid of inclusions. Accessory minerals are essentially twinned loparite and eudialyte. The lowermost zone of the urtite horizon is occupied by an *apatite-bearing juvite* (Ko 97-91, Fig. 4b). This is a leucocratic fine- to medium-grained (1–2 mm) rock with a foliated and porphyritic texture outlined by nepheline phenocrysts (2–5 mm) with subordinate

Table 1

Synthesis of the petrographic and mineralogical compositions of the rocks of unit II-7

Synthetic description of the rocks of unit II-7							
Local name	IUGS nomenclature (Le Maitre, 2002)	Mean thickness	Modal proportions (vol.%)				Principal accessory phases
			alk feld	ne	aeg and arf	Others	
Lujavrite	foid-bearing alkali feldspar syenite	3–4 m	35–80	10–40	10–25	1–3	apatite, loparite
Foyaite	foid syenite	3–4 m	30–40	42–48	7–15	<2	apatite, loparite, titanite (up to 1%), lamprophyllite and murmanite
Juvite	foid syenite	1 m	15–35	45–75	7–15	<2	apatite, loparite
Urtite	ijolite	1 m	5–15	75–85	1–5	2–5	apatite, loparite, eudialyte
Apatite–juvite	apatite-bearing foid syenite	10 cm	10–20	50–60	10–15	7–15	apatite (up to 10%), loparite (ip to 1%)

alk feld: alkali feldspar; ne: nepheline, aeg: aegirine; arf: arfvedsonite.

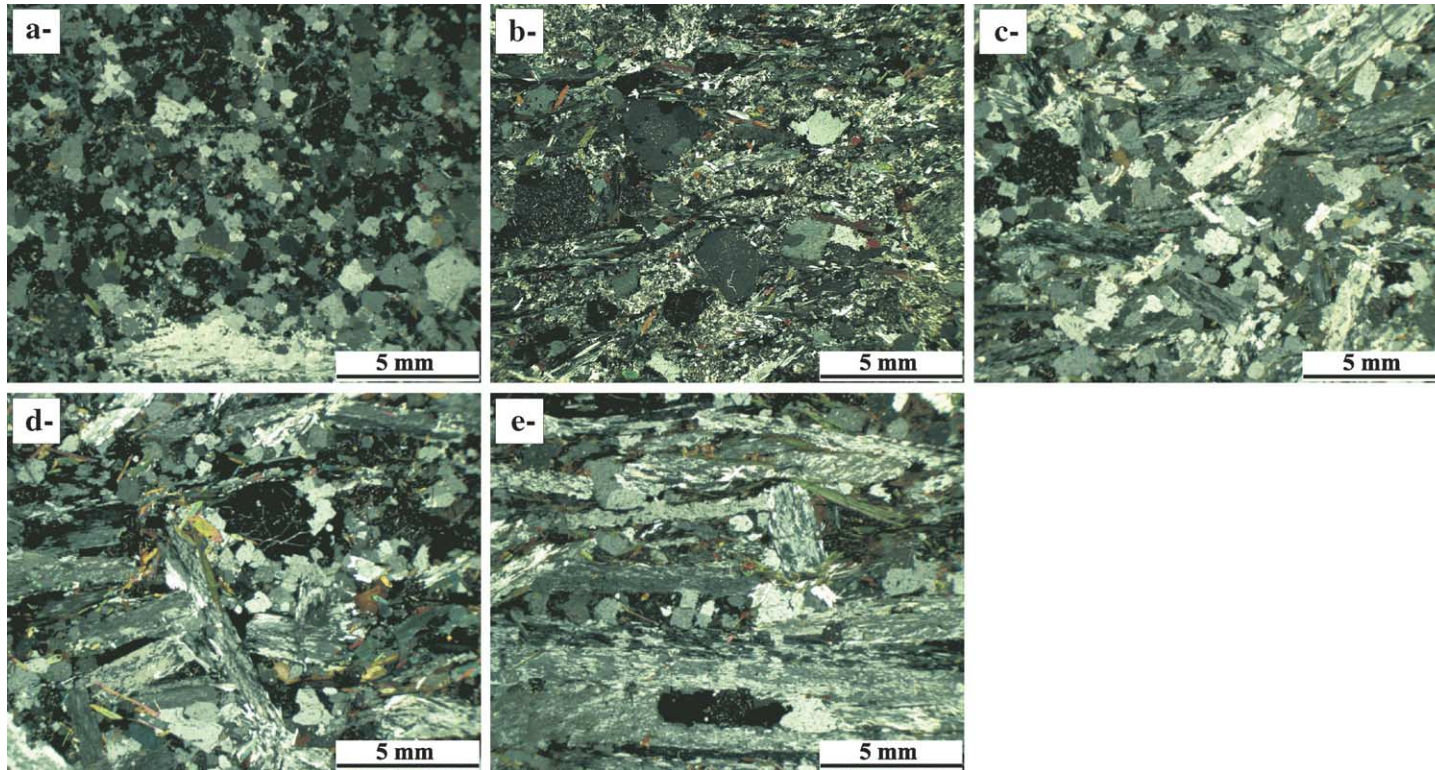


Fig. 4. (a) Medium-grained urtite (Ko 97-92) with rare corroded feldspar laths. Note the consertal texture of nepheline. (b) Fine-grained porphyroidic apatite-bearing juvite (Ko 97-91) showing the solid-state non co-axial C/S (see text) structures near the lower boundary of the unit II-7. Note the pressure shadow features and the strongly weathered matrix. (c) Coarse-grained juvite (Ko 97-95). The alkali feldspar laths (less abundant than in the foyaite) are only slightly interacting. (d) Coarse-grained intersertal foyaite (Ko 97-96) showing a high proportion of interstitial material (nepheline) and the interaction between feldspar laths in a higher liquid proportion. Note the sub-solidus penetration of feldspar ones in others (dissolution–recrystallisation mechanism). (e) Coarse-grained trachytoid lujavrite (Ko 97-99) showing the solid-state non co-axial C/S (see text) structures near the upper boundary of the unit II-7. Note the rotation feature of the feldspar lath in the centre of the micrograph. All photomicrographs (at the same scale) have been cut in the XZ plane. The bar corresponds to 5 mm.

alkali feldspar. The subhedral to euhedral phenocrysts (10–15 vol.%) are set in a fine-grained matrix composed of nepheline and apatite, resulting from the crystallisation of interstitial liquid, and of secondary phases (damourite, sodalite, zeolites) formed by deuteric alteration of silicate phases (nepheline and alkali feldspar). Alkali feldspars are typically perthitic, Carlsbad twinned with late albitic rims. Aegirine is accessory, it occurs as euhedral prisms containing apatite inclusions, it often shows resorption gulfs. Accessory minerals are mainly euhedral loparite and anhedral titanite, in various proportions.

Juvites (i.e. sample Ko 97-95, Fig. 4c) are intermediate rocks between foyaite and urtite; they are leucocratic medium- to coarse-grained (2–5 mm) rocks with a sub-interstitial texture built around euhedral alkali feldspar and sub-euhedral nepheline. They are distinct from urtites by their higher modal abundance of alkali feldspar phenocrysts (up to 35%). Nepheline is also present in the interstitial mineral aggregates where it is polygonal to anhedral; some crystals contain aegirine and apatite inclusions. Prismatic or acicular aegirine (up to 7%) associated with anhedral arfvedsonite (up to 3%) forms aggregates between nepheline and alkali feldspar laths. Loparite and apatite are less abundant (<2%) than in the urtite; eudialyte is rare. Secondary phases (sodalite and zeolites) are observed around feldspar and nepheline.

*Foyaite*s (i.e. sample Ko 97-96, Fig. 4d) are leucocratic medium- to coarse-grained (2–5 mm) rocks with an interstitial texture developed around euhedral alkali feldspar ($\approx 40\%$). The interstices between feldspar laths are occupied by anhedral nepheline (30%) containing numerous aegirine inclusions, arfvedsonite and aegirine in equal proportions and euhedral inclusion-free nepheline ($\approx 15\%$). Euhedral prismatic to subhedral aegirine forms aggregates or occurs in interstitial position or as inclusions in nepheline and feldspar. Arfvedsonite is either poikilitic around nepheline, feldspar and aegirine grains or isolated in the interstices. Interstitial sodalite contains fluid inclusions. Accessory minerals are apatite, anhedral loparite, titanite (up to 1%), lamprophyllite and murmanite.

Lujavrites (i.e. sample Ko 97-99 and Ko 97-93, Fig. 4e) are mesocratic medium- to coarse-grained (2–5 mm) rocks with trachytoid texture outlined by

strong preferred orientation of euhedral alkali feldspar laths. The feldspar modal abundance is comparable or higher (>45%) than in the foyaite while the proportion of mafic phases is higher (up to 20%). Aegirine is prismatic or poikilitic around nepheline, alkali feldspar and loparite. It forms aggregates with anhedral arfvedsonite. Nepheline (20–40%) is subhedral to anhedral, growing in the interstices between feldspar laths. Albite is observed as rims around alkali feldspars, reflecting local post-magmatic albitisation. Sodalite (<5%) may occur in poikilitic structures associated with nepheline. Loparite and apatite are more abundant (1–3%) than in the foyaite, they are either included in nepheline or aggregated. Accessory minerals are eudialyte, murmanite, lorenzenite, titanite and lamprophyllite.

It is important to note that two distinct types of nepheline have been recognised in all rock types: 1) euhedral inclusion-free nepheline occurs mainly in urtites, and as a minor phase in foyaite; 2) anhedral to subhedral inclusion-rich nepheline containing numerous inclusions of aegirine and arfvedsonite, occur in all rock types. Both types are in the size range 0.2 to 0.4 mm; they occur in variable proportions.

3.2. Deformation features

The rocks of the unit II-7 show various, more or less well developed, deformation features illustrated by photomicrographs (Fig. 5) and texture drawing (Fig. 6). These features have been observed in many samples from the central layered part of the massif. However, the understanding of the variations of textures with stratigraphic height has only been possible for the well-exposed unit II-7 (Revda quarry). In fact, our sampling has essentially been made for a petrological–geochemical study both in the quarry and in drill cores. We do not collect orientated samples in the field so that it is not possible to determine the sense and orientation of the deformation features with respect to a geographic reference frame. We nevertheless quantify the fabrics using the intercept method developed by Launeau and Robin (1996). The shape preferred orientation (SPO) ratio R ($R=a/b$, with a and b being the long and short axes of the ellipse respectively) has been obtained by the “INTERCEPT 2003” software on digitalised XZ thin sections (Fig. 6 and Table 2) for the samples from the Revda quarry.

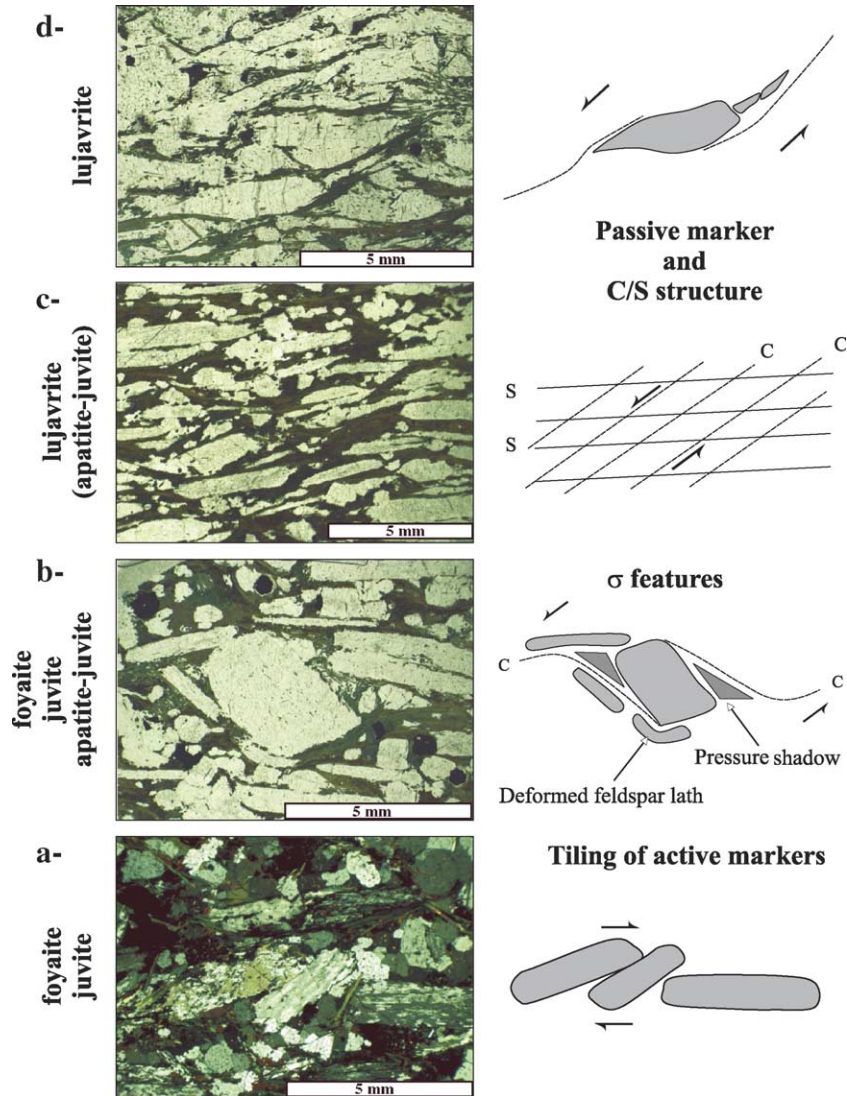


Fig. 5. Some deformation features observed in the rocks of unit II-7. The thin sections have been cut in the XZ plane (perpendicular to the foliation containing the lineation) of the sample. (a) The feldspar laths of the foyaites records the displacement of the particles by tiling of active markers. (b) Rotation of a nepheline phenocryst: the direction of displacement is marked by pressure shadows in an asymmetrical σ feature. Note the torsion of the feldspar laths characterising a sub-magmatic deformation. (c and d) C/S structures in lujavrites: the mean orientation of feldspar laths define the foliation S (or magmatic lamination), whereas the shear bands C are outlined by the pyroxenes and amphiboles. The high modal proportion of feldspar phenocrysts records the high rate of deformation as passive marker.

The basal urtite displays a faint magmatic foliation that is only marked by the rare (but well-oriented) feldspar laths (Fig. 6). Nevertheless, there are too few feldspar laths in the thin section to quantify correctly the SPO. The lowermost rock of the unit, the apatite-bearing juvite (Fig. 4b), presents a fine-grained, highly foliated texture ($R=3.22$; Table 2, Fig. 6): the feldspar laths

and the two types of nepheline (inclusion-free and inclusion-rich) appear as porphyroclasts in a fine-grained matrix essentially composed of secondary phases. Pressure shadow features around phenocrysts and classical C/S structures between them (Berthé et al., 1979; see also explanation of the lujavrite texture) have been observed. The fine-grained matrix displays

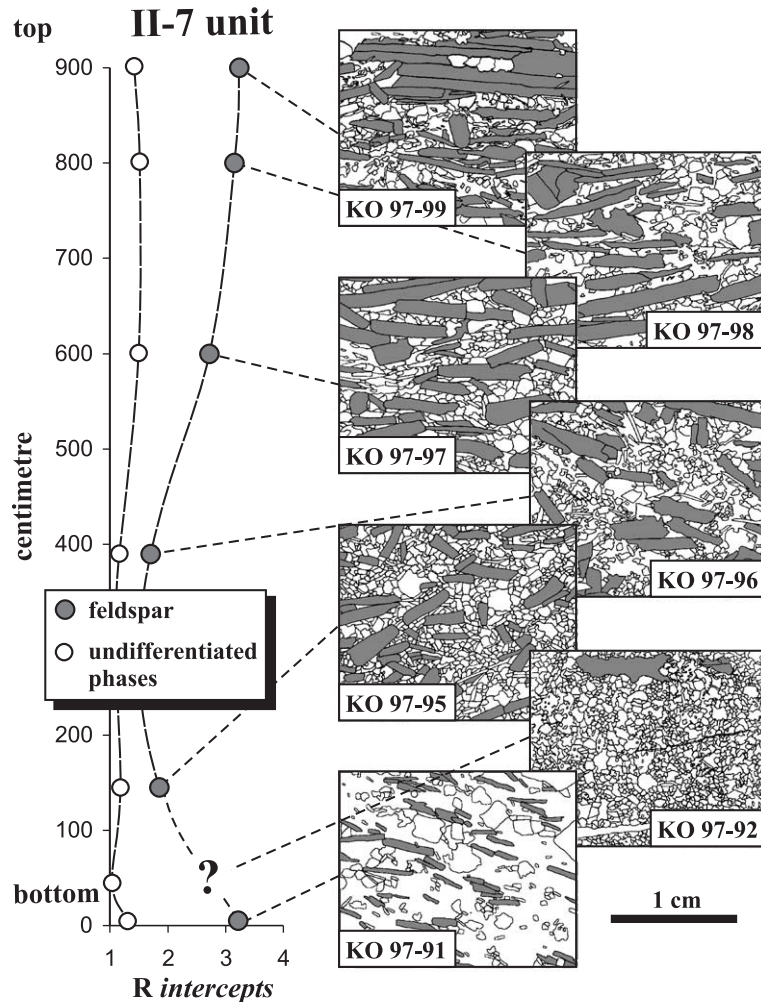


Fig. 6. Stratigraphic variation of the shape preferred orientation (SPO) of feldspar laths and of undifferentiated phases from the matrix (including isometric nepheline) in the complete unit II-7. SPO is given by the ratio R ($R=a/b$, a and b being the long and short axes of the ellipse) obtained by the intercept method developed by Launeau and Robin (1996) ("INTERCEPT 2003" software). The textural evolution is illustrated by drawings of the digitalised XZ thin sections.

a slight SPO ($R=1.31$), locally marked by thin late-magmatic shearing bands.

In juvite and foyaite, the preferred orientation of feldspar laths progressively decreases ($R=1.86$ and 1.71 respectively; Table 2, Fig. 6). Alkali feldspar tiling (Fig. 5a) becomes the dominant structural feature. Isometric nepheline crystals and idiomorphic alkali feldspar laths display sometimes rotation indicators like σ external structures (Passchier and Simpson, 1986) and asymmetrical pressure shadows consisting of a fine-grained deuteritic assemblage between feldspar laths and nepheline (Fig. 5b). In a

given thin section, σ and tiling structures display the same shear sense.

In the lujavrite, the preferred orientation of feldspar laths progressively increases from the central foyaitic zone to the roof, the R parameter varies progressively from 2.72 to 3.24 (Table 2, Fig. 6). Some samples from drill cores also display strong deformation of feldspar laths. The alkali feldspar laths moreover show a crystal shape orientation often characterised by a typical two-planes structure (Fig. 5c and d) – namely crystal orientation planes separated by shear bands – that is

Table 2

Fabric analyses of samples from the unit II-7 as deduced from the shape preferred orientation ratio R

Shape preferred orientation (SPO) for the rocks of unit II-7					
H [cm]	Sample	Rock name	R intercepts ^a , alk feldspar	Modal % ^b , alk feldspar	R intercepts ^c , others
900	Ko 97-99	Lujavrite	3.24	41	1.43
800	Ko 97-98	Lujavrite	3.15	35	1.53
600	Ko 97-97	Lujavrite	2.72	44	1.51
390	Ko 97-96	Foyaite	1.71	33	1.18
145	Ko 97-95	Juvite	1.86	28	1.19
45	Ko 97-92	Urtite	–	5	1.05
5	Ko 97-91	Apatite–Juvite	3.22	11	1.31

^a Shape ratio ($R=a/b$) obtained by the “INTERCEPT 2003” software (Launeau and Robin, 1996) on feldspar laths.^b Modal abundances (vol.%) of alkali feldspar obtained by counting on digitalised thin sections.

comparable (according to the work of Nicolas (1992) on layered gabbros from the Skaergaard intrusion and the Oman ophiolite) to the C/S structure: the foliation “S” (also called the magmatic lamination by Wager and Brown, 1968; Irvine, 1982) and the intersecting shear bands (“C” for “*cisaillement*”, first defined by Berthé et al., 1979). The lujavrites indeed show numerous evidence of plastic strain in crystals (that is in sub-solidus solid state) like fracturing, torsion (i.e. Fig. 5d), mechanical kinks and partial recrystallisation; these features are clearly distinguishable from classical “magmatic” (that is localised in the melt) deformation (Nicolas, 1987, 1989, 1992; Paterson et al., 1998; Bouchez et al., 1992).

Looking at the unit II-7 as a whole (Table 2, Fig. 6), the textural evolution from bottom to top is essentially characterised by the shape preferred orientation of feldspar laths, that display a typical C-shaped profile and by the symmetrical disposition of the anisotropy and shear indicators (C/S, σ , plastic strain of crystals) increasing both near the roof and near the floor of the unit. The other phases (including isometric nepheline) do not show a real orientation because of the weak anisotropy of their crystal shape (i.e. nepheline, loparite...) and/or the strong replacement of primary phases by secondary (post-emplacement) deuteric ones. Nevertheless, the SPO ratios obtained by the intercept method is always slightly higher than 1, illustrating the general prismatic shape of aegirine and/or arfvedsonite crystals around the feldspars.

Table 3a

Selected representative electron microprobe data of the main mineral phases

Feldspar						
Sample	Ko 97-63	Ko 97-63	Ko 97-63	Ko 97-91	Ko 97-91	Ko 97-91
Rock type	Fo	Fo	Fo	Ap Ju II-7	Ap Ju II-7	Ap Ju II-7
Habitus	i ne			i ne		
SiO ₂	64.70	69.20	68.12	68.41	64.21	60.28
TiO ₂	0.05	0.00	0.00	0.00	0.00	0.00
Al ₂ O ₃	18.14	19.77	19.10	19.24	18.24	21.22
Fe ₂ O ₃ calc	0.08	0.09	0.04	0.18	0.01	0.07
MnO	0.00	0.01	0.00	0.00	0.10	0.09
MgO	0.00	0.03	0.00	0.00	0.00	0.00
CaO	0.00	0.02	0.02	0.00	0.00	0.01
BaO	0.05	0.00	0.03	0.13	0.09	0.10
Na ₂ O	0.36	11.75	9.76	11.64	0.44	2.67
K ₂ O	16.78	0.04	3.34	0.17	17.09	15.17
Sum	100.17	100.90	100.41	99.79	100.17	99.61

Formulae based on 8 oxygens

Si	3.00	2.99	3.00	3.00	2.98	2.83
Ti	0.00	0.00	0.00	0.00	0.00	0.00
Al	0.99	1.01	0.99	0.99	1.00	1.17
Fe ³⁺	0.00	0.00	0.00	0.01	0.00	0.00
Mn	0.00	0.00	0.00	0.00	0.00	0.00
Mg	0.00	0.00	0.00	0.00	0.00	0.00
Ca	0.00	0.00	0.00	0.00	0.00	0.00
Ba	0.00	0.00	0.00	0.00	0.00	0.00
Na	0.03	0.99	0.83	0.99	0.04	0.24
K	0.99	0.00	0.19	0.01	1.01	0.91
Ab	3.2	99.7	81.6	99.0	3.7	21.1
Or	96.8	0.2	18.3	1.0	96.3	78.9
An	0.0	0.1	0.1	0.0	0.0	0.0

i ne=inclusion in nepheline.

4. Mineralogy

The main mineral phases that occur sometimes with different habits in the sequence of rocks of unit II-7 have been analysed. The analyses were performed on a Camebax Microprobe at the University of Nancy I (France). The operating conditions were an accelerating voltage of 15 kV, a beam current of 10 nA and a counting time per element of 10 s to 20 s. Standards used were a combination of natural and synthetic minerals. Data correction used a PAP method correction (Pouchou and Pichoir, 1991). Selected representative compositions of the main mineral phases are given in Tables 3a,b,c,d.

All analysed **feldspars** (Table 3a) are strictly alkaline ($An_{0-0.3}$) and display complex perthitic structures (mainly braid perthites) consisting of intimately associated pure albite ($Or_{0-2} Ab_{98-100}$) and microcline ($Or_{92-99} Ab_{1-8}$). Feldspar inclusions in nepheline are also perthitic but their composition

($Or_{79}Ab_{21}$ to $Or_{18}Ab_{82}$) are intermediate between albite and orthoclase and symmetric with respect to the alkali feldspar solvus (Martin and Bonin, 1976). All analysed feldspars are low in Fe_2O_3 (<0.5%) and in BaO (<0.2%).

The composition of the **nepheline** (Table 3b) has been calculated on the basis of 24 cations and 32 atoms of oxygen. The compositional variations of the two types of nepheline described in the petrography section are shown in Fig. 7. The euhedral and inclusion-free nephelines display rather homogeneous compositions ($Ne_{56-68}Ks_{14-19}Q_{15-25}$), characterised by high SiO_2 (44–47.5%) and Fe_2O_3 (1.5–2.4%) contents in comparison with other natural nephelines (see compilation of Dollase and Thomas, 1978). The nepheline inclusions in aegirine and feldspar have compositions comparable to the inclusion-free nephelines. The inclusion-rich nephelines also show quite homogeneous compositions ($Ne_{69-79}Ks_{20-25}Q_{0-11}$) but they are clearly distinct

Table 3b
Selected representative electron microprobe data of the main mineral phases

Nepheline												
Sample	Ko 97-91		Ko 97-93		Ko 97-95		Ko 97-96		Ko 97-99		Ko 97-35	
Rock type	Ap	Ju II-7	Lu II-8	Ju II-7	Fo II-7	Lu II-7	Fo	Fo	Fo	Fo	Fo	Fo
Habitus	Ne 1	Ne 2	Ne 1	Ne 2	Ne 2	Ne 2	i aeg	i aeg	Ne 2	Ne 1	Ne 1	Ne 1
SiO ₂	45.68	43.31	46.05	42.37	42.46	42.65	44.97	44.83	42.65	44.53	45.87	
TiO ₂	0.00	0.00	0.01	0.02	0.00	0.00	0.01	0.00	0.00	0.00	0.00	0.00
Al ₂ O ₃	30.86	33.90	31.40	34.00	33.94	34.00	32.45	30.89	33.48	33.25	31.74	
Fe ₂ O ₃ cal	2.41	0.17	1.68	0.16	0.14	0.18	0.76	2.13	0.30	0.30	1.75	
BaO	0.00	0.00	0.00	0.03	0.00	0.13	0.07	0.11	0.00	0.00	0.00	
Na ₂ O	15.44	15.97	15.70	16.40	16.04	16.23	15.83	15.84	16.22	15.81	15.60	
K ₂ O	5.43	6.89	5.58	7.13	7.57	7.07	5.44	5.60	6.97	6.21	5.45	
CaO	0.00	0.00	0.00	0.00	0.00	0.00	0.00	0.00	0.00	0.00	0.00	
MgO	0.00	0.00	0.00	0.00	0.00	0.00	0.00	0.00	0.00	0.00	0.00	
Sum	99.82	100.25	100.42	100.11	100.16	100.26	99.52	99.42	99.62	100.11	100.42	
<i>Formulae based on 32 oxygens</i>												
Si	8.75	8.32	8.76	8.19	8.21	8.23	8.62	8.66	8.27	8.51	8.72	
Ti	0.00	0.00	0.00	0.00	0.00	0.00	0.00	0.00	0.00	0.00	0.00	
Al	6.97	7.67	7.04	7.75	7.74	7.73	7.33	7.03	7.65	7.49	7.11	
Fe	0.35	0.02	0.24	0.02	0.02	0.03	0.11	0.31	0.04	0.04	0.25	
Ba	0.00	0.00	0.00	0.00	0.00	0.01	0.01	0.01	0.00	0.00	0.00	
Na	5.74	5.95	5.79	6.15	6.02	6.07	5.88	5.93	6.10	5.86	5.75	
K	1.33	1.69	1.35	1.76	1.87	1.74	1.33	1.38	1.73	1.51	1.32	
Ca	0.00	0.00	0.00	0.00	0.00	0.00	0.00	0.00	0.00	0.00	0.00	
Mg	0.00	0.00	0.00	0.00	0.00	0.00	0.00	0.00	0.00	0.00	0.00	
Sum	23.12	23.65	23.18	23.87	23.85	23.80	23.27	23.33	23.79	23.41	23.14	

Rock type: Eu Lu=Eudialyte Lujavrite; Lu=Lujavrite; Fo=Foyaite; Ju=Juvite; Ur=Urtite; Ap Ju=Apatite Juvite.

Ne 1=high T° inclusion free; Ne 2=Low T° inclusion-rich; i aeg=nepheline inclusion in aegirine.

Table 3c
Selected representative electron microprobe data of the main mineral phases

Clinopyroxene															
Sample	Ko 97-1	Ko 97-1	Ko 97-35	Ko 97-35	Ko 97-63	Ko 97-91	Ko 97-93	Ko 97-95	Ko 97-95	Ko 97-96	Ko 97-96	Ko 97-99	Ko 97-99	Ko 97-99	Ko 97-99
Rock type	Fo	Fo	Fo	Fo	Fo	Ap	Lu II-8	Ju II-7	Ju II-7	Fo II-7	Fo II-7	Lu II-7	Lu II-7	Lu II-7	Lu II-7
Habitus	core	rim	core	rim	rim	core	rim	core	i am	core	rim	core	i feld	i ne	rim
SiO ₂	51.49	52.35	50.73	51.77	52.39	51.22	51.95	52.09	52.39	51.68	51.50	52.39	52.41	52.36	53.21
TiO ₂	2.01	2.63	1.48	2.02	1.99	1.59	2.12	1.70	3.03	1.69	2.44	2.41	2.41	0.02	3.69
Al ₂ O ₃	0.85	0.97	0.95	1.11	0.91	0.93	0.95	0.84	1.03	0.94	0.88	0.96	0.99	1.27	0.93
Cr ₂ O ₃	0.00	0.00	0.00	0.00	0.00	0.00	0.00	0.00	0.00	0.00	0.00	0.00	0.00	0.00	0.00
Fe ₂ O ₃ calc	25.88	26.67	24.58	29.10	24.11	23.71	26.21	24.88	26.25	26.03	27.01	26.69	28.68	31.17	21.19
FeO calc	0.88	1.08	0.17	0.00	1.90	1.24	0.00	1.63	1.05	0.19	0.13	0.00	1.28	0.95	4.83
MnO	0.55	0.34	0.50	0.49	0.39	0.53	0.53	0.48	0.58	0.47	0.46	0.50	0.62	0.03	0.63
MgO	2.65	1.29	3.25	0.68	2.15	3.18	2.29	2.49	1.49	3.00	1.66	1.58	0.47	0.08	1.10
CaO	5.13	2.28	7.29	0.49	4.17	6.61	3.53	5.07	2.23	5.73	3.19	3.12	0.79	0.02	1.08
Na ₂ O	10.65	12.32	9.46	13.75	11.11	9.59	11.69	10.76	12.29	10.25	11.47	11.88	13.18	13.19	12.52
K ₂ O	0.00	0.06	0.00	0.04	0.00	0.03	0.06	0.04	0.00	0.00	0.02	0.00	0.02	0.00	0.00
ZrO ₂	0.43	0.40	0.79	0.24	0.53	0.80	0.44	0.30	0.42	0.81	0.98	0.95	0.00	0.11	0.05
Nb ₂ O ₅	0.00	0.00	0.07	0.00	0.00	0.00	0.15	0.00	0.00	0.02	0.04	0.01	0.04	0.00	0.09
Sum	100.52	100.40	99.28	99.69	99.64	99.43	99.93	100.30	100.75	100.80	99.77	100.49	100.88	99.19	99.33

Formulae based on 6 oxygens															
Si	1.956	1.985	1.950	1.981	1.999	1.966	1.976	1.980	1.978	1.955	1.970	1.983	1.984	2.014	2.032
Al ^{IV}	0.038	0.015	0.043	0.019	0.001	0.034	0.024	0.020	0.022	0.042	0.030	0.017	0.016	0.000	0.000
Al ^{VI}	0.000	0.028	0.000	0.031	0.040	0.008	0.018	0.018	0.023	0.000	0.009	0.026	0.028	0.057	0.042
Ti	0.058	0.075	0.043	0.058	0.057	0.046	0.061	0.049	0.086	0.048	0.070	0.069	0.069	0.001	0.106
Cr	0.000	0.000	0.000	0.000	0.000	0.000	0.000	0.000	0.000	0.000	0.000	0.000	0.000	0.000	0.000
Fe ³⁺	0.740	0.761	0.711	0.838	0.692	0.685	0.750	0.712	0.746	0.741	0.777	0.760	0.817	0.902	0.609
Fe ²⁺	0.028	0.034	0.005	0.000	0.061	0.040	0.000	0.052	0.033	0.006	0.004	0.000	0.040	0.031	0.154
Mn	0.018	0.011	0.016	0.016	0.012	0.017	0.017	0.016	0.019	0.015	0.015	0.016	0.020	0.001	0.021
Mg	0.150	0.073	0.186	0.039	0.122	0.182	0.130	0.141	0.084	0.169	0.094	0.089	0.026	0.005	0.063
Ca	0.209	0.093	0.300	0.020	0.170	0.272	0.144	0.207	0.090	0.232	0.131	0.126	0.032	0.001	0.044
Na	0.784	0.906	0.705	1.020	0.821	0.714	0.862	0.793	0.900	0.752	0.850	0.872	0.967	0.984	0.927
Sum	3.98	3.98	3.96	4.02	3.98	3.96	3.98	3.99	3.98	3.96	3.95	3.96	4.00	3.99	4.00

i am=inclusion in amphibole; i feld=inclusion in feldspar; i ne=inclusion in nepheline.

from the inclusion-free nephelines; they are more potassic and less enriched in SiO₂ (<43.5%) and Fe₂O₃ (<0.55%). The excess of Si over that required by stoichiometry can be used as a temperature indicator (Hamilton, 1961). Relative temperatures of crystallisation can indeed be estimated on the basis of the coupled substitutions between Al³⁺ ↔ Si⁴⁺ and Na⁺ ↔ □ in the Ne–Ks solid solution; the experimental isotherms (Greig and Barth, 1938 in Henderson and Gibb, 1983; Hamilton, 1961) have been drawn in Fig. 7. The inclusion-free nephelines crystallise at significantly higher temperatures (>800 °C) than the inclusion-rich nephelines (<700 °C).

The composition of the **clinopyroxenes** (Table 3c), calculated on the basis of four cations and six atoms of oxygen (Morimoto, 1988) is reported for foyaites sampled throughout the whole layered series (Fig. 8a) and for rocks of unit II-7 (Fig. 8b). Pyroxene composition broadly evolves from aegirine-augite to aegirine. For all rock types, the prismatic or large poikilitic crystals of clinopyroxene commonly show normal zoning, with increasing Na and Fe³⁺ and decreasing Ca and Mg contents, from an aegirine-augite core that crystallised at higher temperature than the aegirine rim (Korobeinikov and Laajoki, 1994). The relations between the composition of the pyroxenes in inclusions in other minerals with their host is

Table 3d
Selected representative electron microprobe data of the main mineral phases

Amphibole									
Sample	Ko 97-12	Ko 97-25	Ko 97-35	Ko 97-63	Ko 97-93	Ko 97-95	Ko 97-96	Ko 97-99	Ko 97-99
Rock type	Eu Lu	Fo	Fo	Fo	Lu II-8	Ju II-7	Fo II-7	Lu II-7	Lu II-7
Habitus									i aeg
SiO ₂	52.46	53.41	49.67	50.86	51.17	51.76	51.81	52.11	50.76
TiO ₂	1.47	0.69	2.22	1.84	1.52	1.54	1.60	1.70	1.49
Al ₂ O ₃	1.20	0.78	1.77	2.37	1.67	1.67	1.32	1.44	1.45
Fe ₂ O ₃ calc	2.35	3.24	5.09	4.13	4.65	5.03	2.31	3.54	3.54
FeO calc	15.73	15.34	18.98	12.67	11.22	12.00	18.55	17.27	16.72
MnO	1.59	2.81	2.19	1.73	1.79	1.22	2.15	1.56	2.44
MgO	10.19	9.10	6.03	10.83	11.88	11.78	7.32	8.22	7.91
CaO	1.65	0.44	0.91	2.23	1.90	1.93	0.69	0.90	1.19
Na ₂ O	8.80	8.87	8.49	8.06	8.58	8.59	8.92	8.64	8.63
K ₂ O	1.64	2.39	1.71	1.59	1.63	1.52	1.56	1.72	1.55
F	1.35	0.69	0.02	0.92	1.38	1.82	0.42	1.16	0.01
H ₂ O calc	1.35	1.65	1.93	1.54	1.33	1.15	1.74	1.43	1.93
Sum	99.81	99.44	99.02	98.89	98.77	100.05	98.44	99.87	97.73
–O=F	–0.57	–0.29	–0.01	–0.39	–0.58	–0.77	–0.18	–0.49	–0.01
Sum	99.23	99.14	99.01	98.49	98.18	99.29	98.25	99.38	97.73
<i>Formulae based on 23 oxygens (OH+ F=2)</i>									
Si	7.89	8.07	7.69	7.65	7.70	7.71	7.97	7.89	7.84
Al ^{IV}	0.11	0.00	0.31	0.35	0.30	0.29	0.03	0.11	0.16
Al ^{VI}	0.10	0.14	0.01	0.08	0.00	0.00	0.20	0.15	0.11
Ti	0.17	0.08	0.26	0.21	0.17	0.17	0.18	0.19	0.17
Fe ³⁺	0.27	0.37	0.59	0.47	0.53	0.56	0.27	0.40	0.41
Fe ²⁺	1.98	1.94	2.46	1.59	1.41	1.49	2.39	2.19	2.16
Mn	0.20	0.36	0.29	0.22	0.23	0.15	0.28	0.20	0.32
Mg	2.29	2.05	1.39	2.43	2.66	2.61	1.68	1.86	1.82
Ca	0.27	0.07	0.15	0.36	0.31	0.31	0.11	0.15	0.20
Na	2.56	2.60	2.55	2.35	2.50	2.48	2.66	2.54	2.58
K	0.31	0.46	0.34	0.31	0.31	0.29	0.31	0.33	0.31
F	0.64	0.33	0.01	0.44	0.66	0.86	0.21	0.56	0.01
OH	1.35	1.66	1.99	1.55	1.33	1.14	1.78	1.44	1.99

i aeg=inclusion in aegirine.

quite complex. The aegirines included in arfvedsonite are slightly more Ca-rich than those included in nepheline and alkali feldspar. Inside the unit II-7, there is no significant and systematic variation of pyroxene composition from the base (apatite-bearing juvite) to the top (lujavrite) (Fig. 8b). Moreover within the layered sequence, there is no correlation between the composition of the pyroxenes of the foyaites and the stratigraphic position of the sample. Similar pyroxene trends have been observed in several nepheline syenite occurrences, i.e. Ilimaussaq (Larsen, 1976; Markl et al., 2001), Uganda (Tyler and King, 1967) and Los Islands (Moreau et al., 1996). However, the Lovozero pyroxenes are characterised

by relatively low Mn and Fe²⁺ contents when compared to those of the other massifs.

The compositions of the **amphiboles** (Table 3d), classified according to IMA recommendations (Leake et al., 1997) are calculated on the basis of 13 cations in the tetrahedrally coordinated and C (M1, M2 and M3) sites. In a plot of ^{IV}Al+Ca versus Si+Na+K (Giret et al., 1980), all the amphiboles from the different foyaites of the layered complex as well as those of unit II-7 plot in the arfvedsonite domain (Fig. 9). They commonly show a slight normal zoning with high Mg content in the core to high Fe and Na contents in the rim (core to rim composition: MgO from 10.8% to 8.7%; FeO from

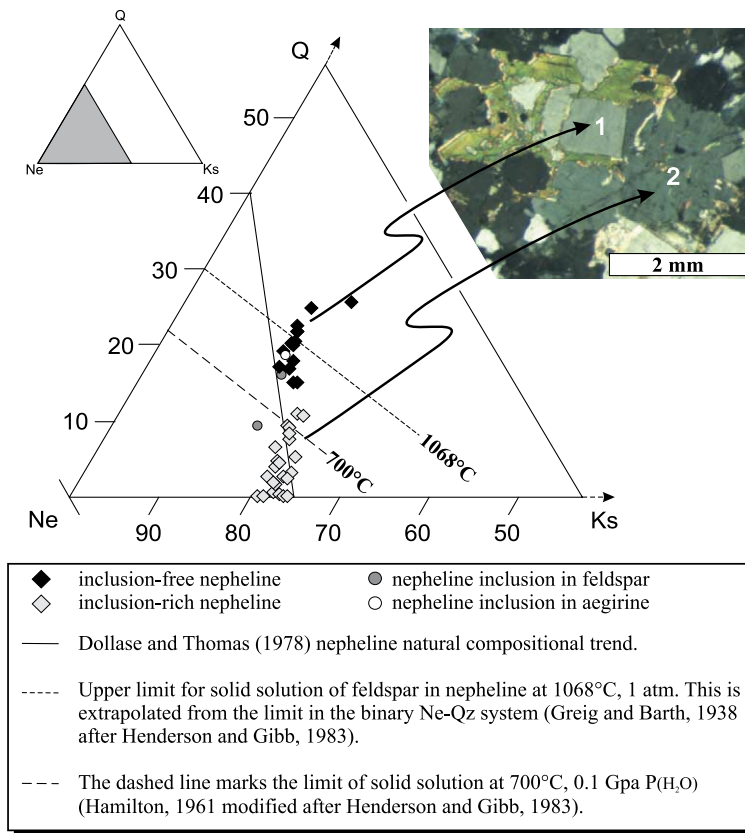


Fig. 7. Nepheline composition (mol%) in the Q-Ne-Ks diagram. Note that the two compositional fields of the Lovozero nephelines do not overlap.

12.7% to 17.5% and Na₂O from 8.1% to 9.2%). Inclusions of arfvedsonite in aegirine are identical to coarse arfvedsonites. The arfvedsonite is systematically more magnesian and less sodic than the aegirine of the same rock. The domain of the Lovozero amphiboles is largely overlapping the fields of amphiboles from the Los Islands agpaite suite (Moreau et al., 1996) and from the Oslo rift plutonic rocks (Neuman, 1976). The Lovozero arfvedsonites are significantly richer in Mg (8 to 11 wt.% MgO) and poorer in Mn (<3 wt.% MnO) than the arfvedsonites from Los Islands (respectively 2.5% MgO and 9% MnO; Moreau et al., 1996).

5. Discussion

The origin of layering in stratiform intrusions remains largely controversial. For peralkaline lay-

ered intrusions like the famous Ilimaussaq and Lovozero, Sørensen (1968) listed the macro-structural features that have to be explained by any mechanism: “a) the rhythmic repetition of mineral-graded units displaying abrupt lower contacts, b) the lateral extent... of almost horizontal layered units, c) the absence of cross-cutting relations..., d) no apparent cryptic layering, e) distinct lamination and cumulus textures” (Sørensen, 1968 p. 269). Some of the layering types of Ilimaussaq appears to be reasonably understood (Larsen and Sørensen, 1987; Sørensen and Larsen, 1987; Upton et al., 1996), but many mechanisms have been proposed to explain the layering of the Lovozero differentiated complex: 1) stratification of the magma in a magma chamber at depth (Bussen and Sakharov, 1967); 2) in situ crystallisation from the roof downwards under static conditions (Vlasov et al., 1959) or from the floor by nepheline accumulation

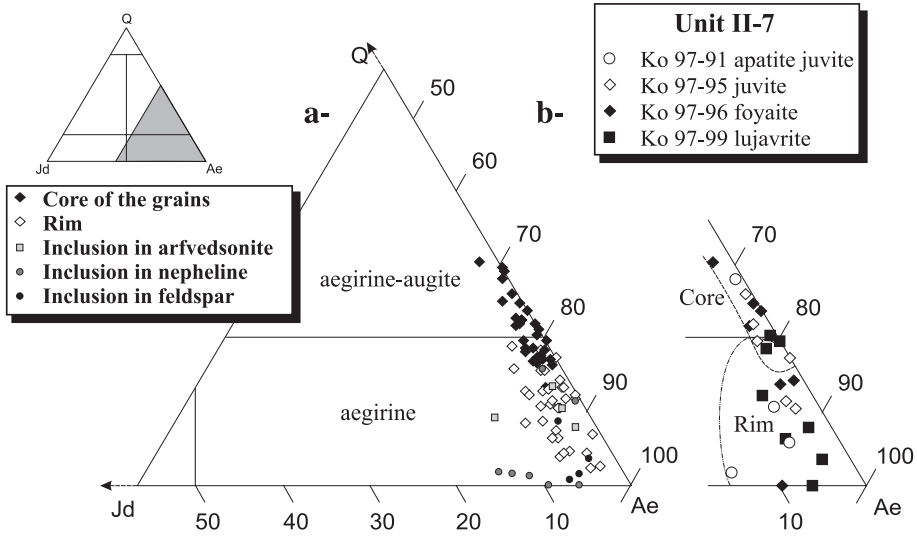


Fig. 8. Compositions of the clinopyroxenes of the Lovozero layered central unit plotted in the Quad–Jadeite–Aegirine diagram (Morimoto, 1988). (a) Pyroxenes of the foyaites throughout the whole layered sequence. Note that the composition of pyroxenes in inclusion largely overlaps the field of rim composition. (b) Pyroxene compositions of rocks of unit II-7. Note the absence of correlation between pyroxene compositions (core and rim) and stratigraphic position in the unit.

(Kogarko and Volkov, 1963; Gerasimovsky et al., 1966) or feldspar flotation (Ivanov, 1960). However, as clearly stated by Sørensen (1968), the crystallisation of a cyclic unit from the early fractionation (of nepheline) to the final eutectic

stage “reflects a high temperature interval (see also Kogarko and Romanchev, 1977) that is difficult to reconcile with the presence of directly overlying, still uncrystallised, magma at higher temperature” (Sørensen, 1968, p. 270).

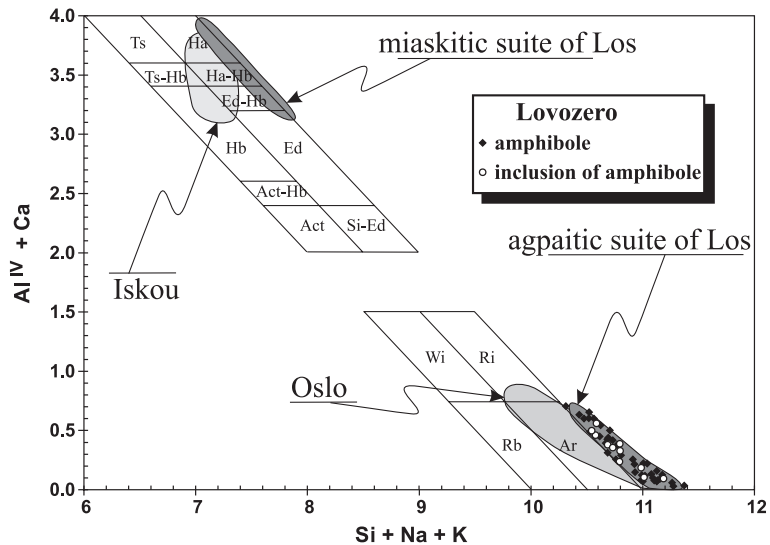


Fig. 9. Composition of the amphiboles of the Lovozero layered central macro-unit plotted in the $Ca + IVAl$ versus $Si + Na + K$ diagram (Giret et al., 1980). The field of arfvedsonite (Ar) from the Oslo Rift (Neuman, 1976), the hastingsite (ha) from the Iskou complex (Giret et al., 1980) and the fields of amphiboles from the miaskitic and agpaitic suites of Los Island (Moreau et al., 1996) are also shown for comparison.

5.1. Cumulus phase versus liquid relationship

The morphology and the textural characteristics of each mineral phase can be discussed in terms of order of crystallisation and of cumulate (=solid) and/or intercumulate (=liquid) growth. In all the rocks of the unit II-7, the alkali feldspar laths (5–7 mm in the urtite to 10–15 mm in the lujavrite) display a euhedral morphology and show evidence of deformation (i.e. fracturing, torsion...) that occurred contemporaneously with the development of the layering (i.e. torsion is observed nearby tiling structure). Moreover, this phase appears as the main element determining the texture of all studied rocks. Thus, it may be considered without ambiguity as a cumulate phase. The status of the nepheline is more complex, as two distinct habits have been recognised in most rocks. The inclusion-free high T nepheline is euhedral and interpreted as a cumulate phase whereas the subhedral to anhedral inclusion-rich low T nepheline most probably crystallised from the interstitial liquid and is thus considered as an intercumulate phase. In the unit II-7, high T nepheline is a minor phase, it represents less than 10% of the total nepheline population. It generally displays a pseudo-isometric (cubic-like) morphology that could result from the destabilisation of a high temperature phase (carnegieite?; Greig and Barth, 1938). Aegirine-augite occurs in the cores of clinopyroxene crystals and as inclusions in low T nepheline; it thus grows after the alkali feldspar and high T , inclusion-free nepheline but before the inclusion-rich nepheline. It could be a cumulate phase characterised by a high nucleation rate but a low growth rate as suggested by its small size and textural occurrence. Aegirine and arfvedsonite crystallize lately, either around the aegirine-augite cores or as large interstitial or poikilitic phases.

Inside the unit II-7, there are strong variations of the cumulus phases/liquid proportions and of the nature of the liquid. The liquid proportion L , estimated from the proportions of intercumulate phases, decreases dramatically from the urtite ($L \approx 90\%$) to the lujavrite ($L \approx 10\%$). The intercumulus assemblage is mainly composed of inclusion-rich low T nepheline and rare ferromagnesian phases in the urtite, whereas in the lujavrite, the proportion of ferromagnesian phases is roughly

equal to that of inclusion-rich nepheline. The interstitial liquid is nepheline-rich at the bottom and more mafic-rich at the top of the unit. Such density inversion of liquid compositions inside a layered unit is commonly observed (even if not easily explained) in other types of cumulates, like for example the anorthosite–leuconorite–norite megacyclic units of the Late Proterozoic Bjerkreim–Sokndal layered intrusion of southwestern Norway (Duchesne, 1972; Wilson et al., 1996).

5.2. Cooling history

Petrographical, mineralogical and textural observations on the rocks of unit II-7 allow us to divide its crystallisation history into 3 stages:

- (1) An initial high temperature stage ($>800\text{ }^{\circ}\text{C}$) characterised by the crystallisation of euhedral to subhedral hypersolvus alkali feldspar, inclusion-free nepheline and aegirine-augite in a magma chamber at depth. The high T of crystallisation of the inclusion-free nepheline (some of them are above the $1068\text{ }^{\circ}\text{C}$ isotherm on Fig. 7) is probably higher than expected for slowly cooled plutons. Kogarko and Romanchev (1977) already reported high experimental crystallisation temperatures for the nephelines of Lovozero. Some nephelines of the augite syenites, sodalite foyaites and kakortokites of the Ilimaussaq layered intrusion have also crystallised at high temperature, in the range $750\text{--}900\text{ }^{\circ}\text{C}$ (Markl et al., 2001). Similar high T of crystallisation for the nepheline syenites of the Chilwa province (Malawi) have been attributed (Woolley and Platt, 1986) to the rapid cooling in a subvolcanic environment. By analogy, it is suggested that the Lovozero complex also crystallised in a subvolcanic magma chamber, implying rapid cooling.
- (2) A second, lower temperature stage ($<700\text{ }^{\circ}\text{C}$) during which the second generation of nepheline, that occurs as subhedral to anhedral inclusion-bearing grains, grew associated with poikilitic aegirine, aegirine rims and inclusions, and arfvedsonite. The crystallisation of a fine-grained matrix occurs during this stage.

Feldspar exsolution (perthitic structure) also probably formed at that stage.

- (3) Locally along the boundaries between units and, to a lesser extent, inside the unit, a strong late- to post-magmatic hydrothermal alteration is observed with most early crystallising silicate phases almost completely transformed into secondary phases (natrolite...). The apatite juvite (Ko 97-91) at the base of the urtite layer is the zone that has been the most profoundly transformed by these hydrothermal fluids.

The layering inside the unit most probably results from magmatic process(es) that occurred during

stage 2 and before the final alteration. During its high-level emplacement, the alkaline magma presumably contained, according to textural evidence (see details below), suspended high T minerals (alkali feldspar, inclusion-free nepheline and some aegirine) in a residual liquid. The mineral/melt relative proportions are about 1/1 in the foyaite; the lujavrite at the top of the unit has a higher proportion of high T minerals while the basal urtite has a high proportion of melt phase. So, our interpretation of the mineral/melt proportions in the different rocks of unit II-7 is qualitatively in agreement with the schematic representation of a cyclic unit provided by [Arzamastsev \(1994\)](#).

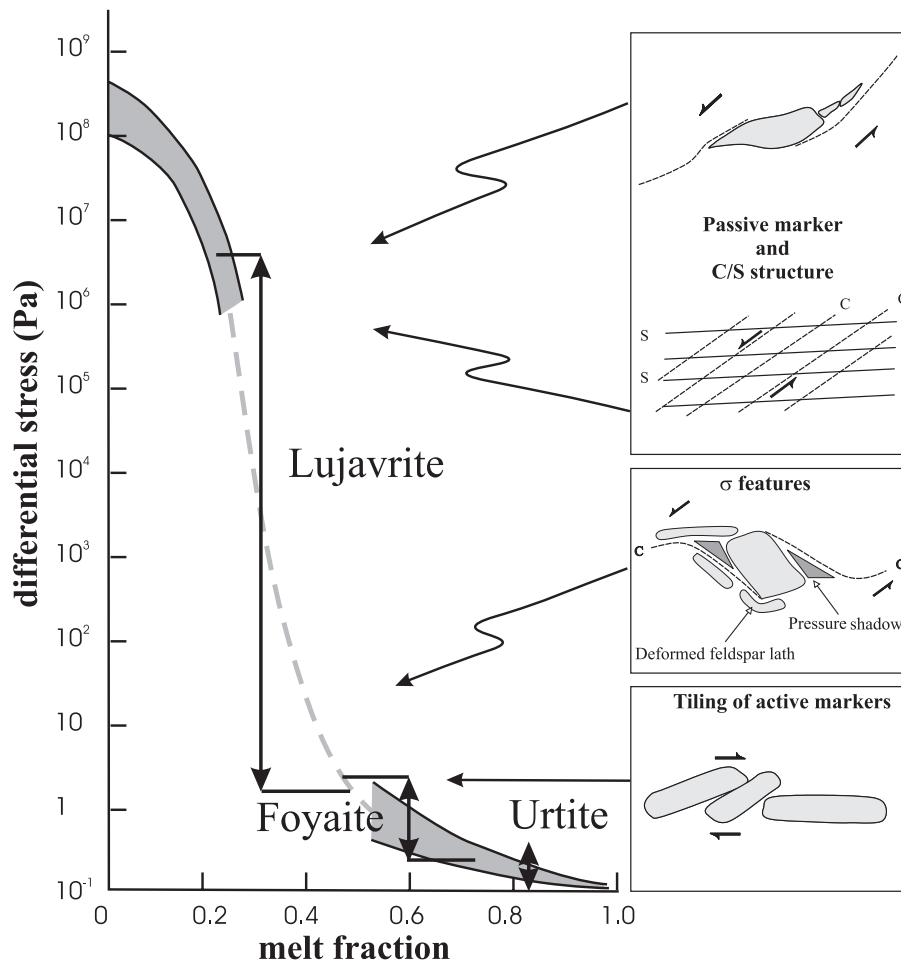


Fig. 10. Relation between the maximum differential stress (in Pa) and the melt fraction (modified after [Wickham, 1987](#) and [Nicolas, 1992](#)). Note that the structural features and the variations of the proportions of cumulus phases and liquid observed in the rocks of the unit II-7 of Lovozero are correlated with the differential stress.

5.3. Localisation and characteristics of the deformation

The textural and modal variations observed in the urtite–juvite–foyaite–lujavrite sequence of unit II-7 can be interpreted by analogy with the experimental results obtained on the distribution and shape orientation of rigid markers (suspended crystals) during magma emplacement (Ildefonse and Fernandez, 1988; Ildefonse et al., 1992; Arbaret et al., 1996, 2001). The rocks of the unit II-7 (from lujavrite to apatite-bearing juvite downwards) and of numerous other units from Lovozero that we have observed (but not described in detail in this paper) show structural features that could be related to the relative modal proportions of suspended crystals and liquid in a non-coaxial simple shear deformation process.

The C/S structures that represent the principal texture of the uppermost (lujavrite) and lowermost (apatite-bearing juvite) layers of the unit II-7 can be related to a shearing plane that is sub-parallel to the

layering. Such structures are characteristic of a nearly solid-state (sub-solidus) deformation event (Nicolas, 1992) affecting magma with a high proportion of crystals, in that case of alkali feldspar (Fig. 10). By contrast, in the foyaite and juvite that occur in the central part of unit II-7, most feldspar laths are oriented in agreement with the rotation of rigid particles (Ildefonse and Fernandez, 1988; Nicolas, 1992) under conditions of low differential stress and relatively high melt fraction; alkali feldspar tiling is the dominant structural feature. All these features develop during a common shearing event related to a planar flow inside the unit; they are not due to the gravitative compaction of a pile of cumulates.

The late solid-state deformation structures (i.e. C/S structures, development of porphyroclasts) observed in the basal apatite-bearing juvite imply that the rock was already nearly completely solidified before deformation occurred. So, to a certain extent, this apatite-bearing juvite could be interpreted as a kind of “chilled margin” corresponding to the extracted liquid

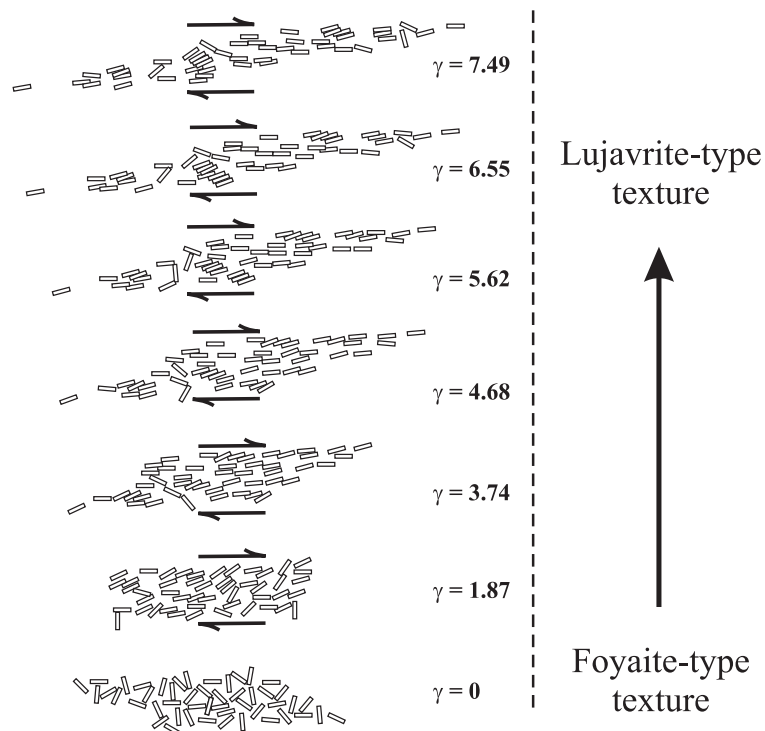


Fig. 11. Two dimensional experiments on orientation during progressive simple shear of identical rigid particles embedded in a weak matrix (Ildefonse and Fernandez, 1988). Note that the textural evolution from the foyaite–juvite to the lujavrite corresponds to an increasing deformation rate γ .

from the crystal mush. This hypothesis could account for the peculiar mineralogical features of this rock: the large, inclusion-rich, nepheline crystals presumably had a higher growth rate than the aegirine, for similar initial nucleation rates. The clinopyroxene and nepheline inclusions are preserved witnesses of the first, high temperature crystallisation stage. Aegirine rims correspond to low temperature overgrowths on the high temperature clinopyroxene (aegirine-augite) core.

For a slight variation of the crystal/melt ratio, the gradation of the shape preferred orientation of feldspar laths (illustrating the finite deformation) from the central foyaite ($R=1.71$) to the lujavrite ($R=3.24$) (Fig. 6) could be linked to an increasing rate of deformation (γ) in the upper part of the unit (as suggested by the analogous experiments of [Ildefonse and Fernandez, 1988](#); Fig. 11). The mechanical concentration (flowage differentiation) of feldspar laths in the uppermost lujavrite occurs during a planar flow in a simple shear that can enhance the assy-

metrical gravitational segregation, as already suggested by [Ivanov \(1960\)](#) and [Upton \(1961\)](#). This mechanism allows to concentrate alkali feldspar laths at the top of the unit while high temperature nepheline with isometric morphology, and to a lesser extent, primary apatite occur all along the profile.

It thus appears that the unit II-7 has to be considered as an independent “structural unit” that cannot be related to the neighbouring overlying and underlying units by simple fractional crystallisation. Moreover, the lack of geochemical differentiation trend for the foyaites sampled throughout the whole layered complex (as exemplified by the clinopyroxene composition; Fig. 8a) for Lovozero also precludes a simple, closed-system, magma chamber evolution contrary to what has been suggested for the Ilimaussaq intrusion ([Engell, 1973](#)). The textures observed in the rocks of unit II-7 and the presence of two generations of crystals suggest a relatively rapid cooling. As the thickness of the sheet of magma that generated unit II-7 (10 to 30 m) and the

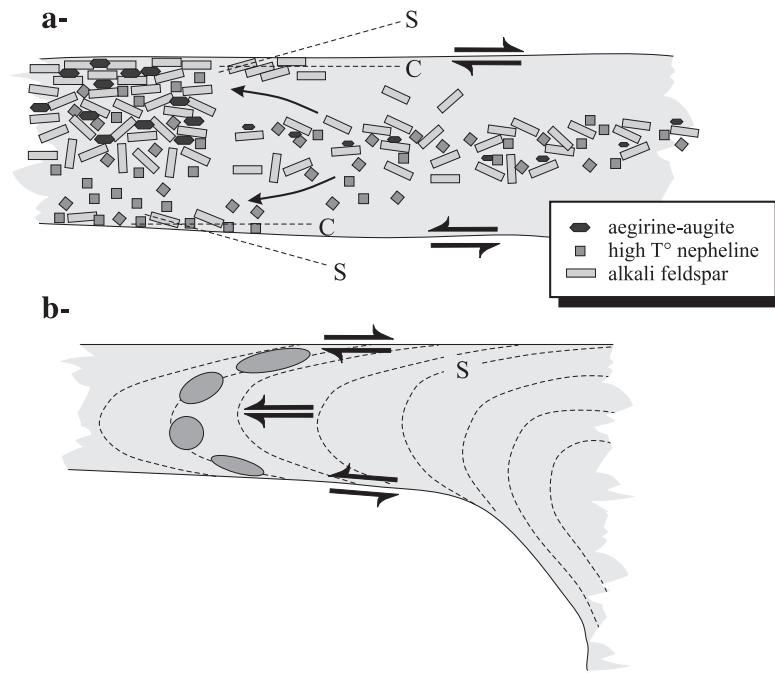


Fig. 12. Sill-like mode of emplacement of the layered unit II-7 illustrated by two theoretical sketches. (a) Schematic synthesis of the petrographic and structural observations. Note the distribution of the “high temperature” minerals (nepheline, alkali feldspar and aegirine) in the unit and the location of the principal non-coaxial simple shear deformation features (C/S, tiling...). For more details, see photomicrographs (Figs. 4 and 5) and text. (b) Schematic model showing the variations of shape fabrics and magmatic foliation S in unit II-7 (see also Fig. 6).

high level of emplacement are similar to those of the Ilmaussaq “en miniature” dyke studied by Marks and Markl (2003), we can use the approach of these authors to constrain the cooling of the Lovozero sill. Whatever the temperature of the enclosing rocks (<150° to 500°), the cooling of the sill would have occurred within a very short time span, in the range 10 to 100 years.

The modal proportions and the spatial arrangement of the mineral phases along the profile of unit II-7 appear to be strongly controlled by kinematics and rapid cooling processes during magma emplacement. Deformational structural features of the different rocks of the complete unit II-7 are in favour of planar flow in a magma sheet, or a sill, associated with a non-coaxial emplacement (lateral flowing) in which sharp boundaries (between the unit and its adjacent rocks) develop and reflect the maximum rate of deformation.

The structural, mineralogical and petrological data of the unit II-7 taken all together suggest that the sheet of magma had a foyaitic mean composition and that it already contained a significant proportion of suspended high temperature mineral phases (Fig. 12). If this sill-like mode of emplacement of unit II-7 can be extended to all the units of the whole layered complex of the Lovozero intrusion, the observed layering could result from a sill-in-sill (or sill-on-sill) process rather than a unique series of intra-magma chamber processes.

6. Conclusion

- 1) The layered part of the Lovozero apgaitic nepheline syenite complex consists of numerous cyclic units. The ideal lithological sequence of unit II-7 is represented, from bottom to top, by urtite–juvite–foyaite–lujavrite.
- 2) Two generations of nepheline have been recognised in most rocks: a high T (>800 °C) inclusion-free nepheline and a low T (<700 °C) inclusion-rich nepheline. Together with perthitic alkali feldspar and aegirine-augite, the high T nepheline belongs to a cumulate assemblage.
- 3) Inside unit II-7, solid-state deformation (C/S texture) and magmatic features (tiling, pressure shadows around active markers) are more prominent in both the upper lujavrite and lower urtite than in the central foyaite. The deformation features can be correlated with the fraction of interstitial liquid remaining.
- 4) The combined textural, mineralogical and petrological data are in favour of the emplacement of unit II-7 as a single pulse of magma with a sheet-like geometry or sill form. The magma was a crystal laden-liquid, presumably of foyaitic composition, already carrying high T crystals from a deeper level magma chamber. The mechanical segregation of crystals occurred during the horizontal flowing of the crystal mush. Solid-state deformation features and compositional gap between high T and low T mineralogies suggest a rapid cooling history of the external part of the sill (roof and floor) during its emplacement. The pulse of magma thus intruded a cold, already largely solidified country-rock and acquired its sill-like structure on rapid cooling.

Acknowledgements

This study has been supported by an INTAS (project No 94-2621) and FNRS-FRFC grants to D. Demaiffe. Thanks are due to Prof. F. Mitrofanov (Kola Centre, Apatity, Russia) who allowed us to study the Kola alkaline province and to Drs V. Nivin, V. Vetrin and E. Balangaskya for the organisation of the fieldtrips. G. Markl is thanked for his thorough and constructive comments on a first draft of this paper. Review by M. Marks, P. Bowden and an anonymous reviewer contribute to significantly improve the manuscript.

References

- Arbaret, L., Diot, H., Bouchez, J.-L., 1996. Shape fabrics of particles in low concentration suspensions: 2D analogue experiments and application to tiling in magma. *J. Struct. Geol.* 18 (7), 941–950.
- Arbaret, L., Mancktelow, N.S., Burg, J.-P., 2001. Effect of shape and orientation on rigid particle rotation and matrix deformation in simple shear flow. *J. Struct. Geol.* 23 (1), 113–125.
- Arzamastsev, A.A., 1994. Unique Paleozoic Intrusions of the Kola Peninsula. Geological Institute of the Kola Science Centre, Apatity. 79 pp.

- Arzamastsev, A.A., 1995. Paleozoic plutonic complexes. In: Mitrofanov, F.P. (Ed.), *Geology of the Kola Peninsula*, pp. 85–103.
- Arzamastsev, A.A., Arzamastseva, L.V., 1995. Alkaline ultrabasic plutonic series of the Lovozero massif, Kola Peninsula. *Trans. (Dokl.) Russ. Acad. Sci.* 348 (4), 533–536.
- Arzamastsev, A.A., Glaznev, V.N., Raevsky, A.B., Arzamastseva, L.V., 2000. Morphology and internal structure of the Kola Alkaline intrusions, NE Fennoscandian Shield: 3D density modelling and geological implications. *J. Asian Earth Sci.* 18, 213–228.
- Atamanov, A.V., Lugov, S.F., Feygin, Y.M., 1961. New results on the geology of the Lovozero Massif (in Russian). *Sov. Geol.* 2, 55–67.
- Balagansky, V.V., Basalae, A.A., Belyaev, O.A., Pozhilenko, V.I., Radchenko, A.T., Radchenko, M.K., 1996. Geological map of the Kola region (north-eastern Baltic shield) scale 1:500,000 (edited by Mitrofanov, F.P., Radchenko, A.T., Gillen, C.), Apatity.
- Beard, A.D., Downes, H., Vertin, V., Kempton, P.D., Maluski, H., 1996. Petrogenesis of Devonian lamprophyres and carbonatites minor intrusions, Kandalaksha Gulf. *Lithos* 39, 93–119.
- Berthé, D., Choukroune, P., Jegouzo, P., 1979. Orthogneiss, mylonite and non-coaxial deformation of granites: the example of the South Armorica Shear Zone. *J. Struct. Geol.* 1, 31–42.
- Bouchez, J.L., Delas, C., Gleizes, C., Nédélec, A., Cuney, M., 1992. Submagmatic microfractures in granites. *Geology* 20, 35–38.
- Bussen, I.V., Sakharov, A.S., 1967. *Geology of Lovozero Tundra* (in Russian). Nauka, Leningrad. 125 pp.
- Cawthorn, R.G. (Ed.), *Layered Intrusions*. Elsevier Science, Amsterdam. 531 pp.
- Dollase, W.A., Thomas, W.M., 1978. The crystal chemistry of silica-rich, alkali-deficient nepheline. *Contrib. Mineral. Petrol.* 66, 311–318.
- Duchesne, J.C., 1972. Iron–titanium oxide minerals in the Bjerkreim–Sokndal massif, south-western Norway. *J. Petrol.* 13, 57–81.
- Engell, J., 1973. A closed system crystal-fractionation model for the agpaaitic Ilimaussaq intrusion, south Greenland with special reference to the lujavrites. *Bull. Geol. Soc. Den.* 22, 334–361.
- Fernandez, A., Febesse, J.L., Mezure, J.F., 1983. Theoretical and experimental study of fabrics developed by different shaped markers in two-dimensional simple shear. *Bull. Soc. Géol. Fr.* 7, 319–326.
- Gerasimovsky, V.I., Volkov, V.P., Kogarko, L.N., Polyakov, A.I., Saprykina, T.V., Balashov, Y.A., 1966. *Geochemistry of the Lovozero Alkaline Massif* (English Translation by Brown D.A. 1968. *Austral. Nation. Univ. Press Canberra*, 369 pp.). Nauka, Moscow. 365 pp.
- Giret, A., Bonin, B., Léger, J.M., 1980. Amphibole compositional trends in oversaturated and undersaturated alkaline plutonic ring-complexes. *Can. Mineral.* 18, 481–495.
- Greig, J.W., Barth, T.F.W., 1938. The system $\text{Na}_2\text{O} \cdot \text{Al}_2\text{O}_3 \cdot 2\text{SiO}_2$ (nepheline, carnegieite)– $\text{Na}_2\text{O} \cdot \text{Al}_2\text{O}_3 \cdot 6\text{SiO}_2$ (albite). *Am. J. Sci.* 35, 93–112.
- Hamilton, D.L., 1961. Nepheline as crystallisation temperature indicator. *J. Petrol.* 69, 321–329.
- Henderson, C.M.B., Gibb, F.G.F., 1983. Felsic mineral crystallization trends in differentiating alkaline basic magmas. *Contrib. Mineral. Petrol.* 84, 355–364.
- Idefonse, B., Fernandez, A., 1988. Influence of the concentration of rigid markers in a viscous medium on the production of preferred orientations. An experimental contribution: 1. Non coaxial strain. *Geological Kinematics and Dynamics* (in Honour of the 70th Birthday of Hans Ramberg), *Bull. Geol. Inst. Univ. Upps.* vol. 14, pp. 55–60.
- Idefonse, B., Launeau, P., Bouchez, J.-L., Fernandez, A., 1992. Effect of mechanical interactions on development of shape preferred orientations: a two-dimensional experimental approach. *J. Struct. Geol.* 14, 74–83.
- Irvine, T.N., 1982. Terminology for layered intrusions. *J. Petrol.* 23, 127–162.
- Ivanov, N.V., 1960. Distribution of minerals in the rocks of the foyaitite–urtite–lujavrite complex of the Lovozero pluton. Problems of geology and mineralogy of the Kola Peninsula (in Russian). *Vopr. Geol. Miner. Kol'sk. Polous.* 3.
- Khomyakov, A.P., 1995. *Mineralogy of Hyperagpaaitic Alkaline Rocks*. Clarendon Press, Oxford. 223 pp.
- Kogarko, L.N., Romanchev, B.P., 1977. Temperature, pressure, redox conditions, and mineral equilibria in agpaaitic nepheline syenites and apatite-nepheline rocks (English translation). *Geokhimiya* 2, 199–216.
- Kogarko, L.N., Volkov, V.P., 1963. Physicochemical evolution of the alkaline magma of the differentiated complex of the Lovozero massif in connection to its rhythmic layering. In: Vinogradov, A.P. (Ed.), *Chemistry of the Earth's Crust* (English Translation: Israel Program for Scientific Translations, Jerusalem, 1966) vol. 1. *Khimiya Zemnoy Kory*, Moscow, pp. 140–152.
- Kogarko, L.N., Kononova, V.A., Orlova, M.P., Woolley, A.R., 1995. *Alkaline Rocks and Carbonatites of the World: Part 2*. Former USSR. Chapman and Hall, London. 225 pp.
- Korobeinikov, A.N., Laajoki, K., 1994. Petrological aspects of the evolution of clinopyroxene composition in the intrusive rocks of the Lovozero alkaline massif. *Geochem. Int.* 31, 33–44.
- Kramm, U., Kogarko, L.N., 1994. Nd and Sr isotope signatures of the Khibina and Lovozero agpaaitic centres, Kola Alkaline Province, Russia. *Lithos* 32, 225–242.
- Kukharev, A.A., Bulakh, A.G., Il'insky, G.A., Shinkarev, N.F., Orlova, M.P., 1967. Mettallogenic peculiarities of alkaline formations of the Eastern Part of the Baltic Shield. *Tr. Leningr. Obš. Estestvoispyt.* 122 (2). (278 pp.).
- Larsen, L.M., 1976. Clinopyroxenes and coexisting mafic minerals from the alkaline Ilimaussaq intrusion, south Greenland. *J. Petrol.* 17, 258–290.
- Larsen, L.M., Sorensen, H., 1987. The Ilimaussaq intrusion–progressive crystallization and formation of layering in an agpaaitic magma. In: Fitton, J.G., Upton, B.G.J. (Eds.), *Alkaline Igneous Rocks*, *Spec. Publ.-Geol. Soc.* vol. 30, pp. 473–488.
- Launeau, P., Robin, P.-Y.F., 1996. Fabric analysis using the intercept method. *Tectonophysics* 267, 91–119.
- Leake, B.E., Woolley, A.R., Arps, C.E.S., Birch, W.D., Gilbert, M.C., Grice, J.D., Hawthorne, F.C., Kato, A., Kisch, H.J., Krivovichev, V.G., Linthout, K., Laird, J., Mandarino, J., Maresch, W.V., Nickel, E.H., Rock, N.M.S., Schumacher,

- J.C., Smith, D.C., Stephenson, N.C.N., Ungaretti, L., Whittaker, E.J.W., Youzhi, G., 1997. Nomenclature of amphiboles: report of the subcommittee on amphiboles of the international mineralogical association commission on new minerals and mineral names. *Min. Mag.* 61, 295–321.
- Le Maitre, R.W. (Ed.), 2002. *Igneous Rocks. A Classification and Glossary of Terms*, 2nd ed. IUGS-Cambridge Univ. Press. 236 pp.
- Markl, G., Marks, M., Schwinn, G., Sommer, H., 2001. Phase equilibria constraints on intensive crystallization parameters of the Ilmaussaq Complex, South Greenland. *J. Petrol.* 42, 2231–2258.
- Marks, M., Markl, G., 2003. Ilmaussaq “en miniature”: closed-system fractionation in an agpaitic dyke rock from the Gardar Province, South Greenland (contribution to the mineralogy of Ilmaussaq no. 117). *Mineral. Mag.* 67, 893–919.
- Martin, R.F., Bonin, B., 1976. Water and magma genesis: the association hypersolvus granite–subsolvus granite. *Can. Mineral.* 14, 228–237.
- Moreau, C., Ohnenstetter, D., Demaiffe, D., Robineau, B., 1996. The Los archipelago nepheline syenite ring-structure: a magmatic marker of the evolution of the central and equatorial Atlantic. *Can. Mineral.* 34, 281–299.
- Morimoto, C., 1988. Nomenclature of pyroxenes. *Mineral. Mag.* 52, 535–550.
- Neuman, E.R., 1976. Compositional relations among pyroxenes, amphiboles and other mafic phases in the Oslo region plutonic rocks. *Lithos* 9, 85–109.
- Nicolas, A., 1987. *Principles of Rock Deformation*. D. Reidel, Dordrecht. 208 pp.
- Nicolas, A., 1989. *Structures of Ophiolites and Dynamics of Ocean Lithosphere*. Kluwer, Dordrecht. 367 pp.
- Nicolas, A., 1992. Kinematics in magmatic rocks with special reference to gabbros. *J. Petrol.* 33 (4), 891–915.
- Osokin, E.D., 1980. Rare-earth Mineralization and Genetic Aspects of the Lovozero Massif Formation. *Ore Geochemistry and Geology of Magmatogenic Deposits*. Nauka, Moscow, pp. 168–178.
- Parsons, I. (Ed.), 1987. *Origins of Igneous Layering*. D. Reidel, Dordrecht. 666 pp.
- Passchier, C.W., Simpson, C., 1986. Porphyroclast systems as kinematic indicators. *J. Struct. Geol.* 8, 831–843.
- Paterson, S.R., Fowler, T.K., Schmidt, K.L., Yoshinobu, A.S., Yuan, E.S., Miller, R.B., 1998. Interpreting magmatic fabric patterns in plutons. *Lithos* 44 (1–2), 53–82.
- Pekov, I.V., 2000. *Lovozero Massif: History, Pegmatites, Minerals*. Ocean Pictures Ltd. 480 pp.
- Pouchou, J.L., Pichoir, F., 1991. Quantitative analysis of homogeneous or stratified microvolumes applying the method “PAP”. In: Heinrich, K.J.F., Newbury, D.E. (Eds.), *Electron Probe Quantification*. Plenum Press, New York, pp. 3–75.
- Sørensen, H., 1968. Rhythmic igneous layering in peralkaline intrusions. An essay review on Ilmaussaq (Greenland) and Lovozero Kola, USSR. *Lithos* 2, 261–283.
- Sørensen, H., 1997. The agpaitic rocks—an overview. *Mineral. Mag.* 61, 485–498.
- Sørensen, H., Larsen, L.M., 1987. Layering in the Ilmaussaq alkaline intrusion, south Greenland. In: Parsons, I. (Ed.), *Origins of Igneous Layering*. D. Reidel, Dordrecht, pp. 1–28.
- Tyler, R.C., King, B.C., 1967. The pyroxenes of the alkaline igneous complexes of eastern Uganda. *Mineral. Mag.* 36, 5–21.
- Upton, B.G.J., 1961. Textural features of some contrasted igneous cumulates from South Greenland. *Medd. Grønl.* 123 (6), 1–31.
- Upton, B.G.C., Parsons, I., Emeleus, C.H., Hodson, C.H., 1996. Layered alkaline igneous rocks of the Gardar Province, South Greenland. In: Cawthorn, R.G. (Ed.), *Layered Intrusions*. Elsevier Science, Amsterdam, pp. 331–363.
- Vlasov, K.A., Kuzmenko, M.Z., Eskova, E.M., 1959. The Lovozero Alkaline Massif (in Russian). *Izd. Acad. Sci., Moscow*. (English translation: Edinburgh: Oliver and Boyd, 1966, 627 pp.)
- Wager, L.R., Brown, G.M., 1968. *Layered Igneous Rocks*. Oliver & Boyd, Ltd., Edinburgh. 558 pp.
- Wager, L.R., Deer, W.A., 1939. *Geological investigations in East Greenland: part 3. The petrology of the Skaergaard intrusion, Kangerdlugssuaq, East Greenland*. *Medd. Grønl.* 105. (335 pp.)
- Wickham, S.M., 1987. The segregation and emplacement of granitic magmas. *J. Geol. Soc. (Lond.)* 144, 281–297.
- Wilson, J.R., Robins, B., Nielsen, F., Duchesne, J.-C., Vander Auwera, J., 1996. The Bjerkreim–Sokndal layered intrusion, Southwest Norway. In: Cawthorn, R.G. (Ed.), *Layering in Igneous Complexes*. Elsevier, Amsterdam, pp. 231–256.
- Woolley, A.R., Platt, R.G., 1986. The mineralogy of nepheline syenite complexes from the northern part of the Chilwa Province, Malawi. *Mineral. Mag.* 50, 597–610.